Supporting information

An Investigation on Hybrid Architecture of Mn-Co Nanoferrite Incorporated in the Polyaniline Matrix for Photoresponse Studies

Anshika Singh[a], Pratima Chauhan[*a], Arpit Verma[b], B. C. Yadav[b]

[a]Advanced Nanomaterials Research Laboratory, U.G.C. Centre of Advanced Studies, Department of Physics, University of Allahabad, Prayagraj-211002, Uttar Pradesh, India

[b]Nanomaterials and Sensors Research Laboratory, Department of Physics, Babasaheb Bhimrao Ambedkar University, Lucknow-226025, U.P., India

1. Mechanism for the formation of MCF-PANI core-shell Nanohybrid

The mechanism of formation and reaction process of MCF-PANI core-shell hybrid nanostructures shown in Figure S1. In the acidic medium, the nano ferrites are positively charged; so, anions (Cl^-) of HCl get adsorbed on the surface of the nano ferrites to compensate for the positive charge.[1, 2] Due to electrostatic interaction between the anions and anilinium cations, aniline monomers are transformed into anilinium cations in process [1]. Thus, the aniline monomers have electrostatically encapsulated the surface of the nano ferrites and polymerized at the temperature 0-5°C in the existence of $(NH_4)_2S_2O_8$ as an oxidizing agent resulting in the formation of core-shell hybrid nanostructured materials.[1, 2]

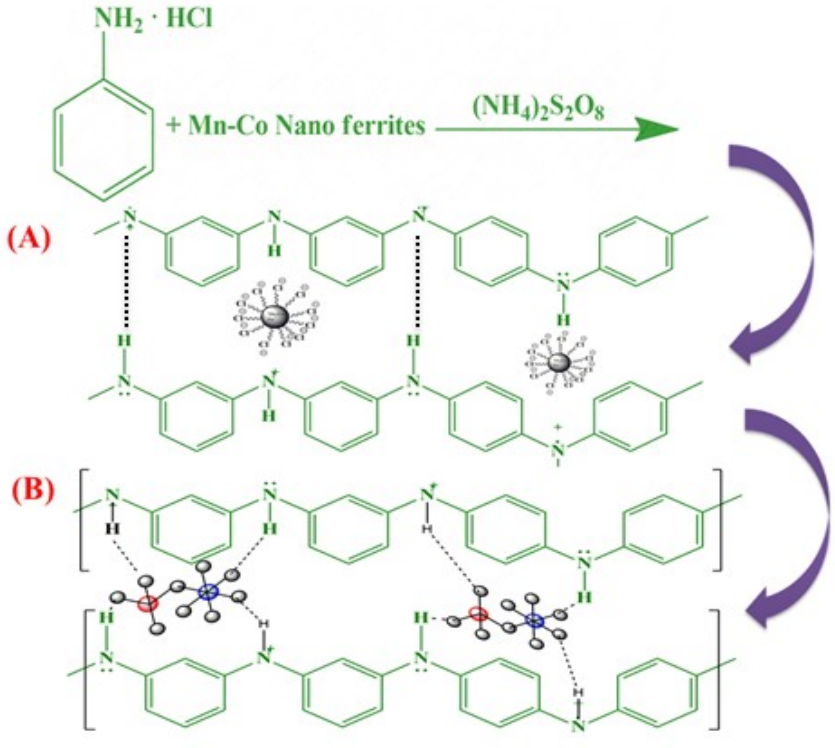

Fig. S1 Reaction mechanism of the formation of core-shell MCF-PANI nanohybrid.

2. X-ray Diffraction

The crystallite size of the material has been calculated by Debye-Scherrer's formula given in the relation (1):

$$\mathbf{D} = \frac{k.\lambda}{\beta cos\,\theta} \quad \textbf{(1)}$$

where D is the average crystallite size, λ is the wavelength of X-ray CuK_{α} (0.154051 nm), and k is constant, which is determined by several factors like the Miller bravais indices and shape of the crystallite often assigned a value of 0.89 considering spherical grains. β is the full width at half maxima (FWHM) of the diffraction peaks measured in radians, and $theta\ is$ Bragg's angle. Lattice parameter 'a' corresponding to the most dominant peak is obtained by using the relation (2):

$$d = \frac{a}{\sqrt{h^2 + k^2 + l^2}} \quad \textbf{(2)}$$

Where d is the interplanar spacing and h, k, and l are the plane's Miller indices.

Interplanar spacing between the lattice plane, 'd', is calculated by using Bragg's law as given in the relation (3):

$$2d\sin\theta = n\lambda \quad \textbf{(3)}$$

Where n is the order of reflection,

All the parameters estimated from the XRD pattern as tabulated in table S1. 2Θ (in degrees), full width half maxima (FWHM), crystallite size (D) and interplanar spacing (d) corresponding to all peaks as given in Table S1. Calculated Average Crystallite Size and Lattice Parameter of as Prepared Samples as given in Table S2.

Table S1 Parameters of the X-ray diffraction pattern of the prepared samples

Materials	2Θ	FWHM	D	Interplanar spacing (d)
MCF	(degree)		(nm)	
	18.44	0.508	16.55	4.805
	30.27	0.419	20.49	2.949

	35.63	0.411	21.16	2.516
	43.29	0.448	19.90	2.087
	45.58	0.332	27.12	1.987
	57.21	0.537	15.69	1.608
	62.83	0.495	19.63	1.477
MCF-PANI Nanohybrid	19.92	16.232	0.52	4.451
	25.15	1.179	7.21	3.536
	29.94	0.235	36.46	2.98
	35.31	0.220	39.53	2.538
	43.23	0.195	45.74	2.09
	53.35	0.455	20.42	1.715
	62.88	0.264	36.76	1.476
PANI	15.17	2.497	3.35	5.833
	20.90	1.006	8.39	4.245
	25.40	1.312	6.48	3.502

Table S2 Calculated average crystallite size and lattice parameter of the prepared samples

Materials	Crystallite size (nm)	Lattice parameter (Å)	Interplanar spacing (Å)
MCF-PANI Nanohybrid	26.66	8.417	2.538
MCF	18.90	8.344	2.516
PANI	15.98	7.004	3.502

3. Scanning electron microscopy (SEM)

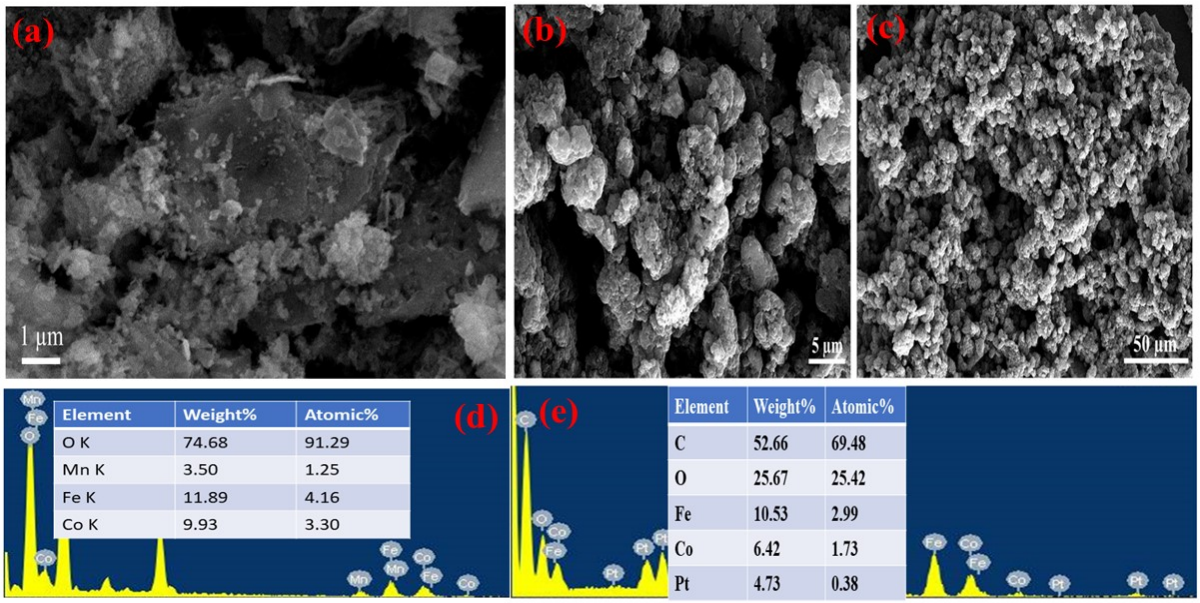

Fig. S2 SEM micrographs of (a) MCF (b and c) MCF-PANI nanohybrid (d) EDAX spectrum of MCF and (e) EDAX spectrum of MCF-PANI nanohybrid with their elemental composition of the sample.

Surface morphological investigations were carried by scanning electron microscope (SEM). A micrograph of MCF at 1 µm shows in Fig. S2a. Randomly stacked irregularly shaped microspheres were observed in the MCF-PANI nanohybrid sample as depicted in Fig. S2(b and c) micrographs possess rough surfaces with porous structures which represent microspherical particles interlinked to each other due to the presence of PANI are clearly shown at 50 µm and 5 µm. EDS spectrum of MCF shown in Fig. S2d with elemental composition. The presence of manganese, cobalt, iron and oxygen was confirmed by the EDS spectrum as given in Fig. S2e. As presented in the EDS spectra, Mn was not detected due to the instrument limitations and platinum is also observed because it was used in the sample preparation.

4. Raman Spectroscopy

All the assignments of the Raman bands of the PANI as given in Table S3 which is same as the bands of the MCF-PANI nanohybrid sample as shown in the manuscript.

Table S3 All the Assignments of Raman Bands of the PANI[3]

Approximate band position (cm^{-1})	Assignments
1640–1644	Phenazine, Phenoxazine, safranine like segments

1620–1623	C–C stretching in B
1597–1603	C–C stretching SQR
1582	C-C stretching in Q
1563–1566	C–C stretching of structures intermediate between Q and SQR
1537	Phenazine, Phenoxazine, safranine-like segments
1530	NH bending
1489	C=N stretching Q
1407	Phenazine like units
1401	Protonated oxazine like units
1396–1397	Phenoxazine like units
1372	$C–N^+$ stretching of SQR, phenosafranine like units
1343–1339, 1320–1323, 1303	$C–N^+$ stretching of radical cations, cyclised structures
1247–1255	C–N stretching in polaronic units
1187–1189	C–H bending B
1166	C–H bending Q
878	Ring def B in ES
775	Ring def Q
748–755	Imine def
603	B ring in plane def
574–575	Ring def, phenoxazine, phenazine like units
515–522	Amine def in pol lattice + CNC torsion in bipolaron
507–509	Out of plane C–H wag
411–414	Out of plane C–H wag in bipolaronic + CNC torsion in polaronic structures

B-benzenoid; Q-quinoid; SQ-semiquinoid rings; def- deformation; ES-emeraldine salt.

Optical Properties

The optical bandgap (E_g) of material is determined with the help of the following relation (4):

$$\alpha h\nu = A(h\nu - E_g)^{\mathbf{n}} \quad \textbf{(4)}$$

where ν is the transition frequency, A is constant, and n = ½ (for direct bandgap). The straight-line portion of the plot was extrapolated to the x-axis, giving the bandgap of the prepared materials.

5. Photoresponse Studies

Time-dependent photoresponse of the MCF photodetector device at the bias voltage of 60 V, 70 V and 90 V as shown in Fig. S2 (a, b and c). The I-V characteristics under illumination

exhibited the predominant linear behavior which is the reminiscent effect of the polarization field. But in metal-semiconductor-metal (MSM) devices the I-V characteristics are generally affected by the two mechanisms such as interfacial and bulk controlled mechanisms. The interfacial mechanism is due to charge injection due to the Schottky effect and bulk controlled a mechanism is contributed to the Ohmic and space charge limited current or the depolarization field. The I-V curve of the MCF photodetector device show curve of power source because it intersects the second quadrant thus current flows out of the positive terminal so electric power flows out of the device into the circuit such as R_{static}= V/I <0. The I-V curves of the MCF photodetector device show a typical behavior of the space charge limited current also. It means that when a high electric field is set up between the electrodes under high drift potential, electrons are ejected from one electrode and goes to the other electrode, so at zero potential there must be non-zero current present in the material shown in Fig. S2d. Time-dependent photoresponse of PANI at the bias voltage of 0.1V, 1V and 5V as shown in Fig. S3 (a, b and c). PANI shows photoresponse of 41.25% at the bias volatage of 5V but MCF doesn't show any response at this voltage. As reported data Mn doped cobalt ferrite nanowires shows excellent performance at the bias voltage of 0.5V.[4] But our MCFs were prepared by easy and chemical approach shows very good photoresponse at 60V. It is clearly seen that the individually MCF can't show that much response so we were chosen MCF with the PANI based MCF-PANI nanohybrid for the photoresponse studies at low voltages. I-V curves for the PANI as shown in the Fig. S4d. All the qualitative parameters of the photodetector device based on MCF-PANI nanohybrid, MCF and PANI as given in the Table S4.

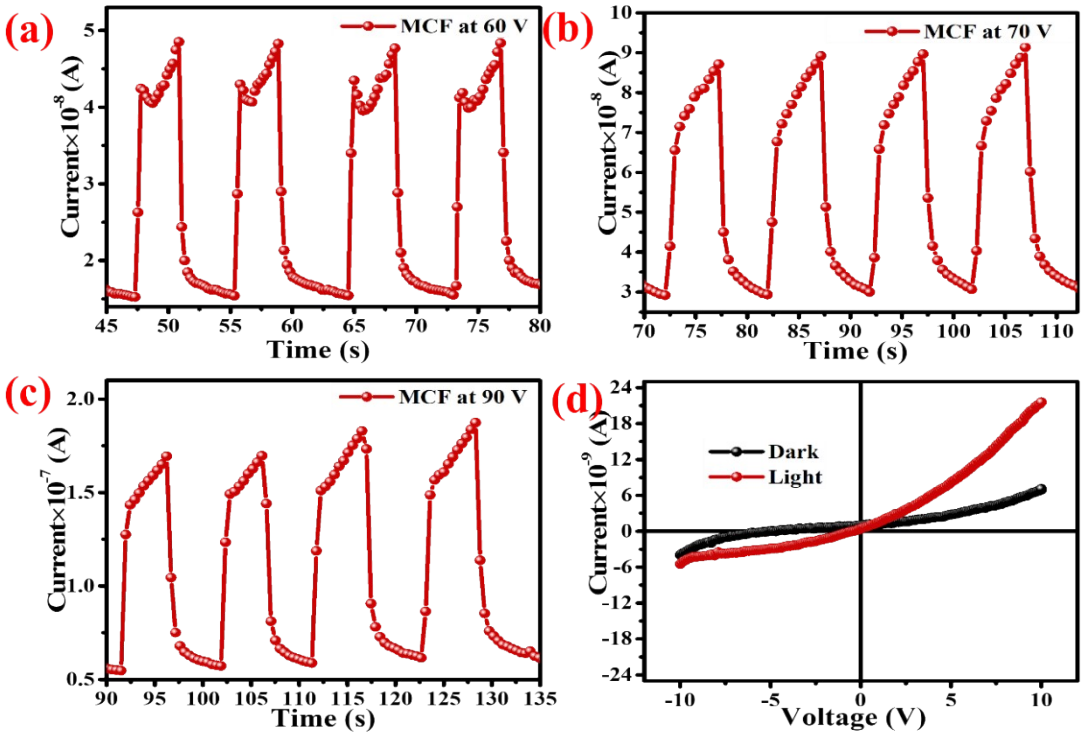

Fig. S3. Photoresponse of MCF at the bias voltage of (a) 60V, (b) 70V (c) 90V (d) I-V curves under light and dark conditions.

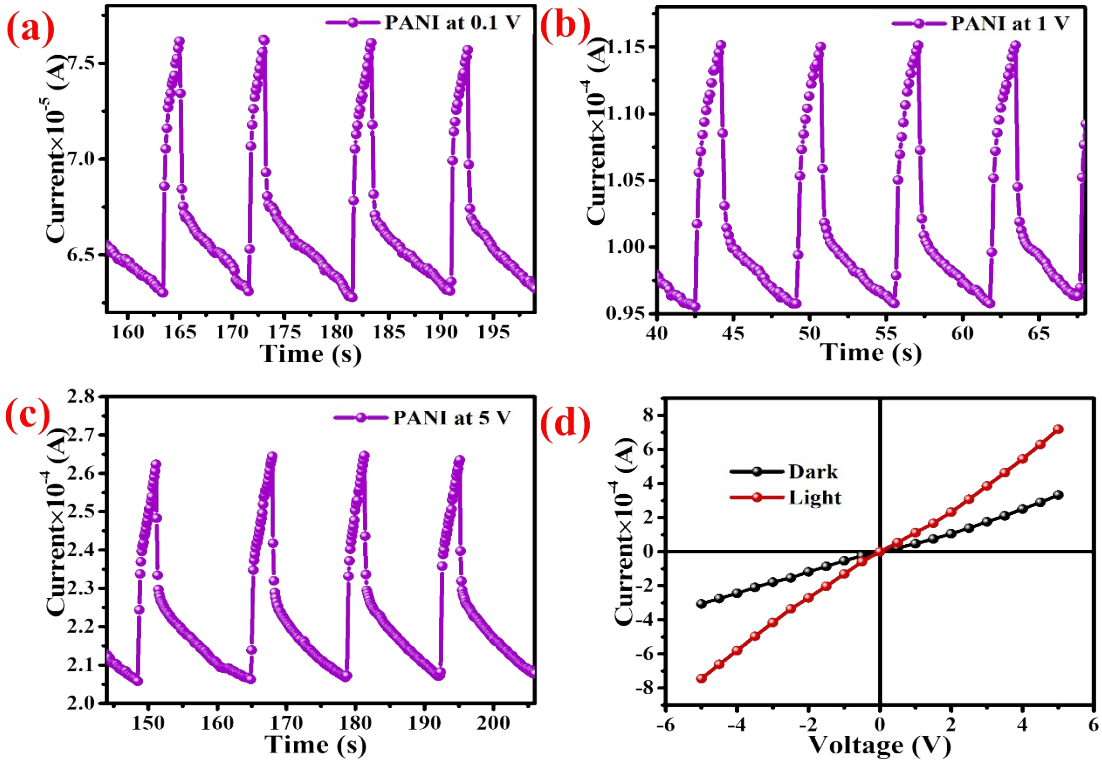

Fig. S4. Photoresponse of PANI at the bias voltage of (a) 0.1V, (b) 1V (c) 5V (d) I-V curves under light and dark conditions.

Table S4 Qualitative parameters of MCF-PANI nanohybrid based photodetector device

Voltage (V)	Responsivity (mAW^{-1})	LDR (dB)	EQE (%)	Detectivity (Jones)	NEP (W)
MCF-PANI Nanohybrid					
0.01	0.004	6.91	120.54	5.41×10^{10}	2.35×10^{-5}
0.1	0.47	7.71	161.60	2.06×10^{11}	2.09×10^{-6}
1	4.66	7.31	1528.18	6.20×10^{11}	2.27×10^{-6}
5	22.69	7.25	7695.07	1.36×10^{12}	2.29×10^{-6}
PANI					
0.1	6.40	14.12	1475.95	2.37×10^{11}	1.44×10^{-5}
1	24.16	8.24	6317.44	8.24×10^{11}	5.13×10^{-6}
5	128.13	6.63	8882.84	8.21×10^{11}	7.27×10^{-6}
MCF					
5	0.0018	9.94	0.63	1.57×10^{10}	7.27×10^{-6}
60	11.03	9.96	3.74	3.84×10^{10}	1.39×10^{-6}
70	19.26	9.45	6.53	4.86×10^{10}	1.52×10^{-6}
90	37.40	9.43	12.68	6.77×10^{10}	1.52×10^{-6}

References

(1) Kotresh, S.; Ravikiran, Y.; Kumari, S. V.; Ramana, C. V.; Anu, A.; Batoo, K. Optimised polyaniline–cadmium ferrite nanocomposite: synthesis, characterisation and alternating current response. *Polymer Bulletin* **2018**, *75* (6), 2475-2490.

(2) Li, L.; Jiang, J.; Xu, F. Novel polyaniline-LiNi0. 5La0. 02Fe1. 98O4 nanocomposites prepared via an in situ polymerization. *European polymer journal* **2006**, *42* (10), 2221-2227.

(3) Xiong, P.; Chen, Q.; He, M.; Sun, X.; Wang, X. Cobalt ferrite–polyaniline heteroarchitecture: a magnetically recyclable photocatalyst with highly enhanced performances. *Journal of Materials Chemistry* **2012**, *22* (34), 17485-17493. Jain, M.; Annapoorni, S. Raman study of polyaniline nanofibers prepared by interfacial polymerization. *Synthetic Metals* **2010**, *160* (15-16), 1727-1732.

(4) Kim, C. H.; Myung, Y.; Cho, Y. J.; Kim, H. S.; Park, S.-H.; Park, J.; Kim, J.-Y.; Kim, B. Electronic structure of vertically aligned Mn-doped $CoFe_2O_4$ nanowires and their application

as humidity sensors and photodetectors. *The Journal of Physical Chemistry C* **2009**, *113* (17), 7085-7090.